View metadata, citation and similar papers at core.ac.uk

brought to you by CORE

provided by Elsevier - Publisher Connector

Alexandria Engineering Journal (2015) 54, 843–851

HOSTED BY

ELSEVIER

Alexandria University

Alexandria Engineering Journal

www.elsevier.com/locate/aej
www.sciencedirect.com

ORIGINAL ARTICLE

Effects of nanoparticles on the peristaltic motion of tangent hyperbolic fluid model in an annulus

S. Nadeem [a], Hina Sadaf [a,*], Noreen Sher Akbar [b]

[a] Department of Mathematics, Quaid-i-Azam University, 45320 Islamabad, Pakistan
[b] DBS&H, CEME, National University of Sciences and Technology, Islamabad, Pakistan

Received 4 November 2013; revised 16 January 2015; accepted 4 July 2015
Available online 23 July 2015

KEYWORDS

Peristaltic flow;
Annulus;
Homotopy perturbation method;
Adomian decomposition method;
Tangent hyperbolic fluid model and comparison

Abstract In the present article, effects of nanoparticles on the peristaltic flow of tangent hyperbolic fluid in an annulus are described. The two-dimensional equations of tangent hyperbolic fluid are solved by using the assumptions of low Reynolds number and long wavelength. Analytical solution is obtained with the help of homotopy perturbation and Adomian decomposition method for velocity, temperature and nanoparticles concentration. Solutions are discussed through graphs. Solutions for pressure rise, temperature, nanoparticles concentration, pressure gradient and streamlines are plotted for various emerging parameters. It is found that the temperature profile increases with increase in Brownian motion and thermophoresis parameter. It is also found that the size of the trapped bolus in triangular wave is smaller as compared to other waves. Further, the comparison of both analytical solutions is presented.

© 2015 Faculty of Engineering, Alexandria University. Production and hosting by Elsevier B.V. This is an open access article under the CC BY-NC-ND license (http://creativecommons.org/licenses/by-nc-nd/4.0/).

1. Introduction

Peristalsis is a distinct pattern of smooth muscle contractions that mix the food material properly through the esophagus and intestines. Literature on peristalsis is quite extensive i.e. with the initiative work of Latham [1], in which he discussed the fluid motion in peristaltic pump. After Latham, Jaffrin and Shapiro [2] made developments on mathematical modeling and experimental fluid mechanics of peristaltic flows. They made analysis under the assumption of long wavelength and low Reynolds number approximation. Peristaltic motion in both mechanical and physiological situations has been discussed by various researchers in the past few years [3–8]. Recently, peristaltic flow has gained much attention of the researchers due to its wide range of applications in physiology and industries [9–13].

Nanofluid is basically the liquid suspension that contains tiny particles of diameter less than 100 nm. These particles can be found in metals such as, oxides, carbides, nitrides or nonmetals (Graphite, carbon nanotubes). The pioneering work for nanofluids was reported by Choi [14], who observed that the small amount of these nanoparticles significantly increases the thermal conductivity of the base fluid. Buongiorno [15] presented convective transport in nanofluids, where he proposed a nonhomogeneous equilibrium model which predicts that increase in the thermal conductivity occurs due to the presence of the Brownian motion and thermophoretic parameters, which are basically the diffusion of nanoparticles. Kuznetsov and Nield [16] reported the natural convective

* Corresponding author.
E-mail address: hsqau@hotmail.com (H. Sadaf).

Peer review under responsibility of Faculty of Engineering, Alexandria University.

http://dx.doi.org/10.1016/j.aej.2015.07.003

1110-0168 © 2015 Faculty of Engineering, Alexandria University. Production and hosting by Elsevier B.V.
This is an open access article under the CC BY-NC-ND license (http://creativecommons.org/licenses/by-nc-nd/4.0/).

boundary layer flow of nanofluid past a rigid flat plate. Sadik and Pramuanjaroenkij [17] discussed the review of convective heat transfer enhancement with nanofluids. Two-dimensional boundary layer flow of nanofluid over an impermeable stretching sheet was analyzed by Khan and Pop [18]. Heat transfer enhancement by using nanofluids in forced convection flows was visualized by Marga et al. [19]. Rana and Bhargava [20] extended the work of Khan and Pop for nonlinearly stretching sheet. The influence of endoscope on the peristaltic transport of nanofluid has been examined by Akbar and Nadeem [21]. Analysis of nanoparticles on peristaltic flow of Prandtl fluid model in an endoscope has been addressed by Nadeem et al. [22]. Recently, a theoretical study of Prandtl nanofluid in a rectangular duct through peristaltic transport is presented by Ellahi et al. [23].

The current research is conducted to study the effects of nanoparticles on peristaltic flow of tangent hyperbolic fluid in an annulus. The two-dimensional equations of tangent hyperbolic fluid are solved by using the assumptions of low Reynolds number and long wavelength. Analytical solution is obtained with the help of homotopy perturbation and Adomian decomposition methods for velocity, temperature and nanoparticles concentration. Graphical results are presented for pressure rise, pressure gradient, stream function, temperature and nanoparticles concentration. Interpretation is presented with respect to interesting parameters entering into the problem.

2. Model of the problem

Governing equations for an incompressible non-Newtonian nanofluid model are defined as [21,22]

$$\operatorname{div}\overline{\mathbf{A}} = 0, \tag{1}$$

$$\rho_f \frac{d\overline{\mathbf{A}}}{d\bar{t}} = \operatorname{div}\overline{\mathbf{S}} + \rho_f \mathbf{f}, \tag{2}$$

$$(\rho c)_f \frac{d\overline{T}}{d\bar{t}} = k\nabla^2\overline{T} + (\rho c)_p\left[D_B \nabla\overline{C}.\nabla\overline{T} + \left(\frac{D_{\overline{T}}}{\overline{T}_1}\right)\nabla\overline{T}.\nabla\overline{T}\right], \tag{3}$$

$$\frac{d\overline{C}}{d\bar{t}} = D_B\nabla^2\overline{C} + \left(\frac{D_{\overline{T}}}{\overline{T}_1}\right)\nabla^2\overline{T}, \tag{4}$$

where $\overline{\mathbf{A}}$ is the velocity component, $\overline{\mathbf{S}}$ gives the Cauchy stress tensor, $\overline{C}$ the nanoparticles concentration, D_B the Brownian diffusion coefficient and $D_{\overline{T}}$ the thermophoretic diffusion coefficient respectively. Constitutive equation of tangent hyperbolic fluid is defined as [11]

$$\overline{\mathbf{S}} = -\overline{P}\mathbf{I} + \bar{\tau}, \tag{5}$$

$$\bar{\tau} = [[\eta_\infty + (\eta_{0+}\eta_\infty)\tanh(\Gamma\dot{\bar{\gamma}})^m]\dot{\bar{\gamma}}_i], \tag{6}$$

in which $\bar{\tau}$, η_0, η_∞, m, Γ, denote the extra stress tensor, zero shear rate viscosity, infinite rate of shear viscosity, power law index, time constant respectively and $\dot{\bar{\gamma}}$ is now defined as

$$\dot{\bar{\gamma}} = \sqrt{\frac{1}{2}\sum_i\sum_j \dot{\bar{\gamma}}_{ij}\dot{\bar{\gamma}}_{ji}} = \sqrt{\frac{1}{2}\pi}, \tag{7}$$

where

$$\boldsymbol{\pi} = trace(grad\ \overline{\mathbf{A}} + (grad\ \overline{\mathbf{A}})^T)^2, \tag{8}$$

in which π is the second invariant strain tensor. We study Eq. (6) in the case for $\eta_\infty = 0$ and $\Gamma\dot{\bar{\gamma}} < 1$. The element of extra stress tensor therefore is inscribed as

$$\bar{\tau} = \eta_0[(\Gamma\dot{\bar{\gamma}})^m]\dot{\bar{\gamma}}_i = \eta_0[(1+\Gamma\dot{\bar{\gamma}}-1)^m]\dot{\bar{\gamma}}_i = \eta_0[1+m(\Gamma\dot{\bar{\gamma}}-1)]\dot{\bar{\gamma}}_i, \tag{9}$$

$$\dot{\bar{\gamma}}_i = \mathbf{L} + \mathbf{L}^T. \tag{10}$$

3. Formulation of the problem

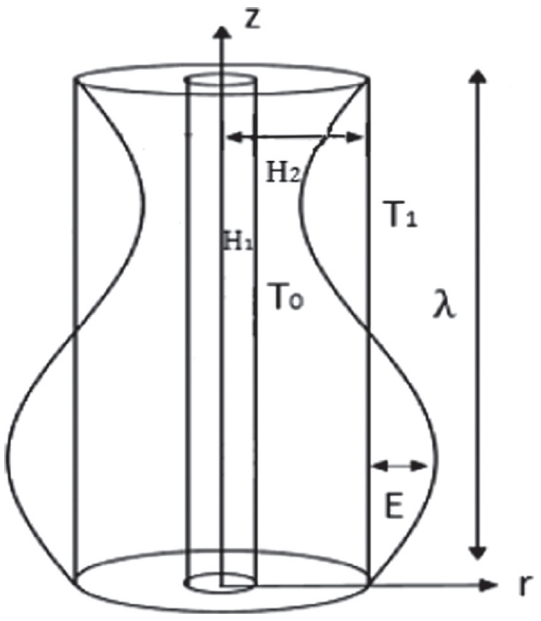

Geometry of the problem

Considering the peristaltic transport in the profile of an incompressible tangent hyperbolic fluid in an annulus. Inward cylinder is rigid, and kept at temperature $\overline{T}_0$; however, outward cylinder takes a sinusoidal wave traveling down its walls and kept at temperature $\overline{T}_1$. Wall surface geometry is expressed as

$$\overline{R}_1 = H_1, \tag{11}$$

$$\overline{R}_2 = H_2 + E\sin\frac{2\pi}{\lambda}(\overline{Z} - s\bar{t}), \tag{12}$$

where H_1, H_2, λ, E, s are the radius of the inward and outward cylinders, wave length, wave amplitude and wave speed respectively. The governing equations in the fixed frame for two-dimensional incompressible tangent hyperbolic fluid model in the presence of nanoparticles are given as

$$\frac{\partial\overline{U}}{\partial\overline{R}} + \frac{\overline{U}}{\overline{R}} + \frac{\partial\overline{W}}{\partial\overline{Z}} = 0, \tag{13}$$

$$\rho_f\left(\frac{\partial\overline{U}}{\partial\bar{t}} + \overline{U}\frac{\partial\overline{U}}{\partial\overline{R}} + \overline{W}\frac{\partial\overline{U}}{\partial\overline{Z}}\right) = -\frac{\partial\overline{P}}{\partial\overline{R}} + \frac{1}{\overline{R}}\frac{\partial(\overline{R}\bar{\tau}_{\overline{RR}})}{\partial\overline{R}} + \frac{\partial(\bar{\tau}_{\overline{TR}})}{\partial\overline{Z}}, \tag{14}$$

$$\rho_f\left(\frac{\partial\overline{W}}{\partial\bar{t}} + \overline{U}\frac{\partial\overline{W}}{\partial\overline{R}} + \overline{W}\frac{\partial\overline{W}}{\partial\overline{Z}}\right) = -\frac{\partial\overline{P}}{\partial\overline{Z}} + \frac{1}{\overline{R}}\frac{\partial(\overline{R}\bar{\tau}_{\overline{RZ}})}{\partial\overline{R}} + \frac{\partial(\bar{\tau}_{\overline{ZZ}})}{\partial\overline{Z}} + \rho_f g\alpha_{\overline{T}}(\overline{T}-\overline{T}_1) + \rho_f g\alpha_{\overline{C}}(\overline{C}-\overline{C}_1), \tag{15}$$

$$\left(\frac{\partial\overline{T}}{\partial\bar{t}} + \overline{U}\frac{\partial\overline{T}}{\partial\overline{R}} + \overline{W}\frac{\partial\overline{T}}{\partial\overline{Z}}\right) = \alpha_f\left(\frac{\partial^2\overline{T}}{\partial\overline{R}^2} + \frac{1}{\overline{R}}\frac{\partial\overline{T}}{\partial\overline{R}} + \frac{\partial^2\overline{T}}{\partial\overline{Z}^2}\right) + \tau_1\left\{D_B\left(\frac{\partial\overline{C}}{\partial\overline{R}}\frac{\partial\overline{T}}{\partial\overline{R}} + \frac{\partial\overline{C}}{\partial\overline{Z}}\frac{\partial\overline{T}}{\partial\overline{Z}}\right) + \frac{D_{\overline{T}}}{\overline{T}_1}\left[\left(\frac{\partial\overline{T}}{\partial\overline{R}}\right)^2 + \left(\frac{\partial\overline{T}}{\partial\overline{Z}}\right)^2\right]\right\}, \tag{16}$$

$$\left(\frac{\partial\overline{C}}{\partial\bar{t}} + \overline{U}\frac{\partial\overline{C}}{\partial\overline{R}} + \overline{W}\frac{\partial\overline{C}}{\partial\overline{Z}}\right) = D_B\left(\frac{\partial^2\overline{C}}{\partial\overline{R}^2} + \frac{1}{\overline{R}}\frac{\partial\overline{C}}{\partial\overline{R}} + \frac{\partial^2\overline{C}}{\partial\overline{Z}^2}\right) + \frac{D_{\overline{T}}}{\overline{T}_1}\left(\frac{\partial^2\overline{T}}{\partial\overline{R}^2} + \frac{1}{\overline{R}}\frac{\partial\overline{T}}{\partial\overline{R}} + \frac{\partial^2\overline{T}}{\partial\overline{Z}^2}\right), \tag{17}$$

In the above equations, $D_{\overline{T}}$ the thermophoretic diffusion coefficient, D_B and the Brownian diffusion coefficients of mass diffusivity $\tau_1 = \frac{(\rho c)_p}{(\rho c)_f}$ which depicts the ratio of the effective heat capacity in the case of nanoparticle material and heat capacity of the fluid. In the fixed coordinates $(\overline{R}, \overline{Z})$, the flow in the cylinders is unsteady, and it converts steady in a wave frame $(\bar{r}, \bar{z})$ moving with same speed as the wave moves in the $\overline{Z}$ directions. The conversions between the wave references are [24]

$$\bar{r} = \overline{R},\ \bar{z} = \overline{Z} - s\bar{t},\ \bar{u} = \overline{U},\ \bar{w} = \overline{W} - s, \tag{18}$$

In the wave reference $\bar{u}$ and $\bar{w}$ are the velocity components. The boundary limits are expressed as

$$\begin{aligned}
&\bar{w} = -s,\ \text{at } \bar{r} = \bar{r}_1,\ \bar{w} = -s \text{ at } \bar{r} = \bar{r}_2 = H_2 + E\sin\frac{2\pi}{\lambda}(\bar{z}),\\
&\overline{T} = \overline{T}_0 \text{ at } \bar{r} = \bar{r}_1,\ \overline{T} = \overline{T}_1 \text{ at } \bar{r} = \bar{r}_2,\\
&\overline{C} = \overline{C}_0 \text{ at } \bar{r} = \bar{r}_1,\ \overline{C} = \overline{C}_1 \text{ at } \bar{r} = \bar{r}_2.
\end{aligned} \tag{19}$$

Introducing the dimensionless variables

$$\begin{aligned}
&R = \frac{\overline{R}}{H_2},\ r = \frac{\bar{r}}{H_2},\ W = \frac{\overline{W}}{s},\ w = \frac{\bar{w}}{s},\ Z = \frac{\overline{Z}}{\lambda},\ z = \frac{\bar{z}}{\lambda},\ U = \frac{\lambda\overline{U}}{H_2 s},\\
&u = \frac{\lambda\bar{u}}{H_2 s},\ t = \frac{s\bar{t}}{\lambda},\ P = \frac{H_2^2\overline{P}}{s\lambda\eta},\ \theta = \frac{\overline{T} - \overline{T}_1}{\overline{T}_0 - \overline{T}_1},\ \hat{\delta} = \frac{H_2}{\lambda},\ Re = \frac{\rho_f s H_2}{\eta},\\
&S = \frac{H_2\overline{S}}{s\eta},\ r_1 = \frac{\bar{r}_1}{H_2} = \frac{H_1}{H_2} = \in,\ r_2 = \frac{\bar{r}_2}{H_2} = 1 + \phi\sin\ 2\pi z,\\
&We = \frac{\Gamma s}{H_2}, \alpha_f = \frac{k}{(\rho c)f},\ N_b = \frac{(\rho c)_p D_B(\overline{C}_0 - \overline{C}_1)}{(\rho c)_f \alpha_f},\\
&N_t = \frac{(\rho c)_p D_{\overline{T}}(\overline{T}_0 - \overline{T}_1)}{(\rho c)_f \overline{T}_1 \alpha_f}, G_r = \frac{\rho_f g \alpha_{\overline{T}} H_2^2(\overline{T}_0 - \overline{T}_1)}{\eta s},\\
&B_r = \frac{\rho_f g \alpha_{\overline{C}} H_2^2(\overline{C}_0 - \overline{C}_1)}{\eta s},\ \phi = \frac{E}{H_2},\ \tau = \frac{\overline{\tau} H_2}{\eta s}\\
&\dot{\gamma} = \frac{H_2}{s}\bar{\dot{\gamma}},\ \sigma = \frac{\overline{C} - \overline{C}_1}{\overline{C}_0 - \overline{C}_1}.
\end{aligned} \tag{20}$$

We define N_t, B_r, Re, G_r, We, N_b, $\hat{\delta}$, $\phi < 1$, $\alpha_{\overline{T}}$, $\alpha_{\overline{c}}$, are the thermophoresis parameter, local nanoparticle Grashof number, Reynolds number, local temperature Grashof number, Weissenberg number, Brownian motion parameter, wave number, ϕ is the amplitude ratio, coefficient of thermal expansion, and coefficient of expansion with nanoconcentration respectively. Using Eqs. (18) and (20) into Eqs. (13)–(17), we obtain

$$\frac{\partial u}{\partial r} + \frac{u}{r} + \frac{\partial w}{\partial z} = 0, \tag{21}$$

$$\hat{\delta}^3 Re\left(u\frac{\partial u}{\partial r} + w\frac{\partial u}{\partial z}\right) = -\frac{\partial p}{\partial r} + \hat{\delta}^2\frac{\partial}{\partial z}(\tau_{rz}) + \frac{\hat{\delta}}{r}\frac{\partial}{\partial r}(r\tau_{rr}), \tag{22}$$

$$\hat{\delta} Re\left(u\frac{\partial u}{\partial r} + w\frac{\partial w}{\partial z}\right) = -\frac{\partial p}{\partial z} + \frac{1}{r}\frac{\partial}{\partial r}(r\tau_{rz}) + \hat{\delta}\frac{\partial}{\partial r}(\tau_{zz}) + G_r\theta + B_r\sigma, \tag{23}$$

$$\frac{1}{r}\frac{\partial}{\partial r}\left(r\frac{\partial\theta}{\partial r}\right) + N_b\frac{\partial\sigma}{\partial r}\frac{\partial\theta}{\partial r} + N_t\left(\frac{\partial\theta}{\partial r}\right)^2 = 0, \tag{24}$$

$$\left(\frac{1}{r}\frac{\partial}{\partial r}\left(r\frac{\partial\sigma}{\partial r}\right)\right) + \frac{N_t}{N_b}\left(\frac{1}{r}\frac{\partial}{\partial r}\left(r\frac{\partial\theta}{\partial r}\right)\right) = 0, \tag{25}$$

where

$$\tau_{rr} = 2\hat{\delta}[1 + m(We\dot{\gamma} - 1)]\frac{\partial u}{\partial r}, \tag{26}$$

$$\tau_{rz} = [1 + m(We\dot{\gamma} - 1)]\left(\frac{\partial u}{\partial z}\hat{\delta}^2 + \frac{\partial w}{\partial r}\right), \tag{27}$$

$$\tau_{zz} = 2\hat{\delta}[1 + m(We\dot{\gamma} - 1)]\frac{\partial w}{\partial z}, \tag{28}$$

$$\dot{\gamma} = \left[2\hat{\delta}^2\left(\frac{\partial u}{\partial r}\right)^2 + \left(\frac{\partial u}{\partial z}\hat{\delta}^2 + \frac{\partial w}{\partial r}\right)^2 + 2\hat{\delta}^2\left(\frac{\partial w}{\partial z}\right)^2 + 2\hat{\delta}^2\frac{u^2}{r^2}\right]^{\frac{1}{2}}. \tag{29}$$

We note that Eqs. (22) and (23) are non-linear; therefore, we are interested to solve our problem incorporating the suppositions of low Reynolds number and long wavelength, avoiding the terms of order $\hat{\delta}$ and greater, and Eqs. (22)–(25) take the following form

$$\frac{\partial p}{\partial r} = 0, \tag{30}$$

$$\frac{\partial p}{\partial z} = \frac{1}{r}\frac{\partial}{\partial r}\left(r\left([1 + m(We\dot{\gamma} - 1)]\left(\frac{\partial w}{\partial r}\right)\right)\right) + G_r\theta + B_r\sigma, \tag{31}$$

$$\frac{1}{r}\frac{\partial}{\partial r}\left(r\frac{\partial\theta}{\partial r}\right) + N_b\frac{\partial\sigma}{\partial r}\frac{\partial\theta}{\partial r} + N_t\left(\frac{\partial\theta}{\partial r}\right)^2 = 0, \tag{32}$$

$$\left(\frac{1}{r}\frac{\partial}{\partial r}\left(r\frac{\partial\sigma}{\partial r}\right)\right) + \frac{N_t}{N_b}\left(\frac{1}{r}\frac{\partial}{\partial r}\left(r\frac{\partial\theta}{\partial r}\right)\right) = 0. \tag{33}$$

Eq. (30) illustrates that p is not a function of r. The resultant dimensionless boundary limits for the problem under concern are given as

$$\begin{aligned}
&w = -1 \text{ at } r = r_1,\ w = -1 \text{ at } r = r_2 = 1 + \phi\sin(2\pi z),\\
&\sigma = \theta = 1 \text{ at } r = r_1,\ \sigma = \theta = 0 \text{ at } r = r_2,
\end{aligned} \tag{34}$$

4. Analytical solutions

4.1. Homotopy perturbation solution

To obtain the solution of above equations, we used homotopy perturbation method. The homotopy perturbation method suggests [25–31] that we write Eqs. (31)–(33), as

$$H(j,\sigma) = (1-j)[\pounds(\sigma) - \pounds(\sigma_{20})] + j\left[\pounds(\sigma) + \frac{N_t}{N_b}\left(\frac{1}{r}\frac{\partial}{\partial r}\left(r\frac{\partial\theta}{\partial r}\right)\right)\right], \tag{35}$$

$$H(j,\theta) = (1-j)[\pounds(\theta) - \pounds(\theta_{20})] + j\left[\pounds(\theta) + N_b\frac{\partial\theta}{\partial r}\frac{\partial\sigma}{\partial r} + N_t\left(\frac{\partial\theta}{\partial r}\right)^2\right], \tag{36}$$

$$\begin{aligned}
&H(j,w) = (1-j)[\pounds(w) - \pounds(w_{20})]\\
&+ j\left[\pounds(w) - \frac{\partial p}{\partial z} + \frac{1}{r}\frac{\partial}{\partial r}\left(rmWe\left(\frac{\partial w}{\partial r}\right)^2\right) + G_r\theta + B_r\sigma\right].
\end{aligned} \tag{37}$$

The linear operator and the initial guesses are chosen as

$$\begin{aligned}
&\pounds_{\theta r} = \frac{1}{r}\frac{\partial}{\partial r}\left(r\frac{\partial}{\partial r}\right),\ \pounds_{\sigma r} = \frac{1}{r}\frac{\partial}{\partial r}\left(r\frac{\partial}{\partial r}\right),\ \pounds_{wr} = \frac{1}{r}\frac{\partial}{\partial r}\left(r(1-m)\frac{\partial}{\partial r}\right),\\
&\sigma_{20}(r,z) = \left(\frac{r - r_2}{r_1 - r_2}\right),\ \theta_{20}(r,z) = \left(\frac{r - r_2}{r_1 - r_2}\right),\\
&w_{20} = -1 + \frac{dp_0}{dz}\left(\frac{r^2}{4(1-m)} + \ell_{49}\ln(r) + \ell_{50}\right).
\end{aligned} \tag{38}$$

According to HPM, we define

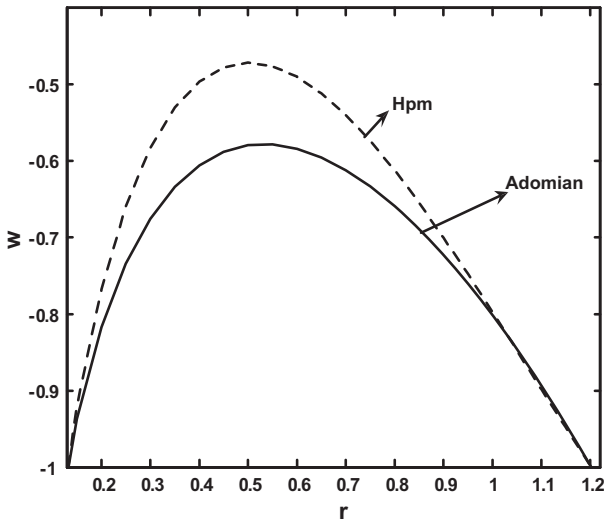

Fig. 1 Velocity field for $m = 0.27, N_t = 1.22, G_r = 2.46, B_r = 2.43, N_b = 4.86, We = 0.12, \quad Q = 0.01, \varepsilon = 0.13, \phi = 0.25, z = 0.15$.

$$\begin{aligned}
\theta &= \theta_0 + j\theta_1 + j^2\theta_2 + \ldots, \\
\sigma &= \sigma_0 + j\sigma_1 + j^2\sigma_2 + \ldots, \\
w &= w_0 + jw_1 + j^2w_2 + \ldots, \\
F_i &= F_{oi} + jF_{1i} + j^2F_{2i} + \ldots
\end{aligned} \tag{39}$$

With the help of above equations, Eqs. (35)–(37) after equating the like powers of j and summarizing the perturbation results for parameter $j \to 1$, the expression for nanoparticles concentration, temperature and velocity profile can be written as

$$\sigma = \ell_{28}r^2 + r\ell_{36} + \ell_{37}\ln r + \ell_{38}, \tag{40}$$

$$\theta = \ell_{39}r^3 + r^2\ell_{46} + \ell_{41}r + \ell_{47}\ln r + \ell_{48}, \tag{41}$$

$$\begin{aligned}
w = {} & -1 + \frac{dp}{dz}\left(\frac{r^2}{4(1-m)} + \ell_{49}\ln r + \ell_{50}\right) \\
& + r^4\ell_{68} + r^3\ell_{79} + r^2\ell_{80} + r\ell_{81} + \frac{1}{r}\ell_{82} - \frac{\ell_{75}}{r^2} \\
& + \ell_{83}\ln r + \ell_{73}r^2\ln r + \ell_{84},
\end{aligned} \tag{42}$$

in which all ℓ_{ij} are defined in Appendix A.

The expression for pressure gradient can be obtained as

$$\frac{dp}{dz} = \frac{F_i}{\ell_{86}} + \ell_{89}. \tag{43}$$

Flow rate in dimensionless form is defined as

$$Q = F_i + \frac{1}{2}\left(1 + \frac{\phi^2}{2} - \varepsilon^2\right). \tag{44}$$

The expressions for dimensionless time mean flow rate F_i, Pressure rise Δp and friction forces (at the wall) on the outward and inward cylinders are F^a and F^b respectively

$$\Delta p = \int_0^1 \left(\frac{dp}{dz}\right)dz,\ F^a = \int_0^1 -r_1^2\left(\frac{dp}{dz}\right)dz,\ F^b = \int_0^1 -r_2^2\left(\frac{dp}{dz}\right)dz. \tag{45}$$

The velocities and stream function relation are defined as

$$u = \frac{-1}{r}\left(\frac{\partial\Psi}{\partial z}\right) \text{ and } w = \frac{1}{r}\left(\frac{\partial\Psi}{\partial r}\right). \tag{46}$$

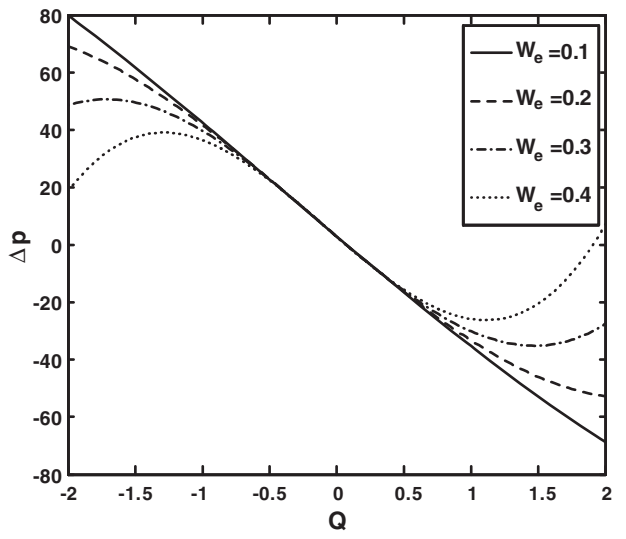

Fig. 2 Pressure rise versus flow rate for, $m = 0.1, \phi = 0.05, N_b = 2.41, N_t = 5.14, G_r = 3.32, B_r = 2.22, \varepsilon = 0.02$.

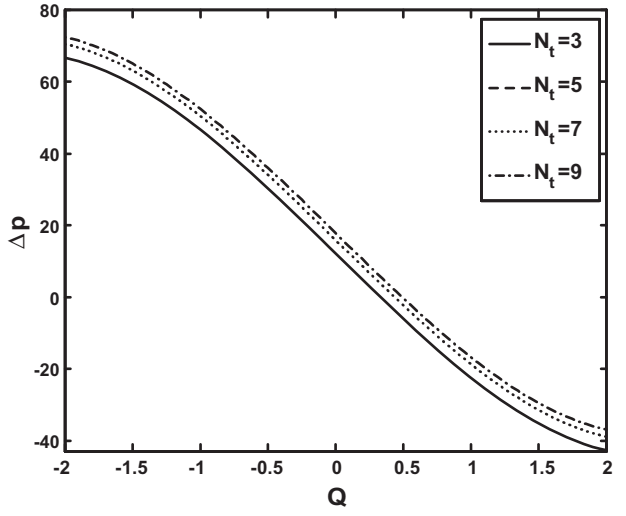

Fig. 3 Pressure rise versus flow rate for $\phi = 0.03, \varepsilon = 0.01, We = 0.14, B_r = 3.62, m = 0.11$.

For study, we considered four waveforms explicitly, sinusoidal, triangular, trapezoidal, and square wave, and dimensionless expression can be stated as

1. Sinusoidal wave:

$$r_2(z) = 1 + \phi\sin(2\pi z). \tag{47}$$

2. Triangular wave:

$$r_2(z) = 1 + \phi\left\{\frac{8}{\pi^3}\sum_{y=1}^{\infty}\frac{(-1)^{y+1}}{(2y-1)}\sin(2\pi(2y-1)z)\right\}. \tag{48}$$

3. Trapezoidal wave:

$$r_2(z) = 1 + \phi\left\{\frac{32}{\pi^2}\sum_{y=1}^{\infty}\frac{\sin\frac{\pi}{8}(2y-1)}{(2y-1)^2}\sin(2\pi(2y-1)z)\right\}. \tag{49}$$

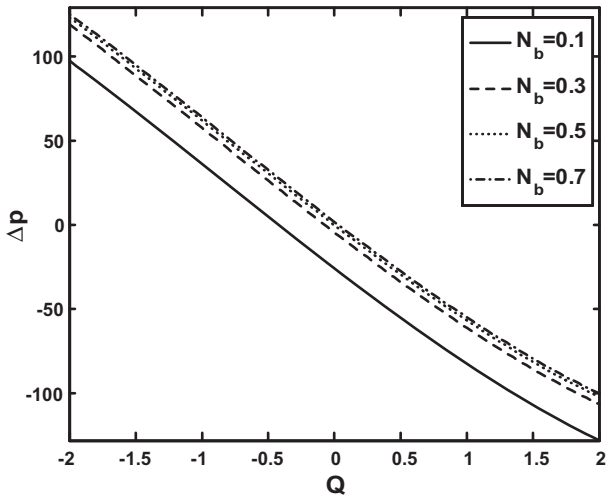

Fig. 4 Pressure rise versus flow rate for $\phi = 0.03, \varepsilon = 0.01$, $We = 0.14, B_r = 3.62, m = 0.11$.

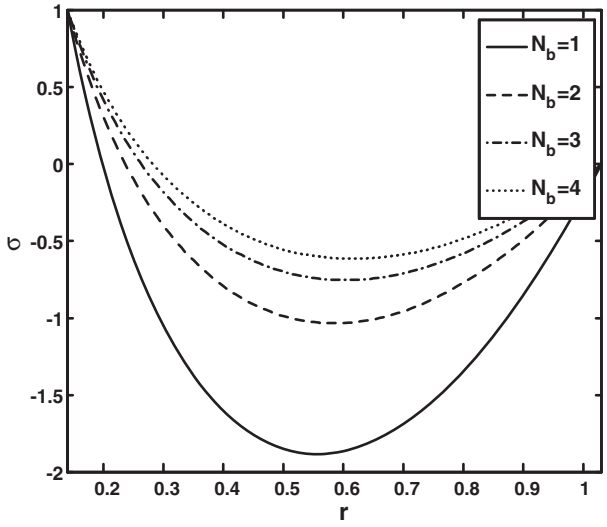

Fig. 6 Nanoparticles concentration profile for $z = 0.26$, $\phi = 0.03, \varepsilon = 0.14, N_t = 3.55$.

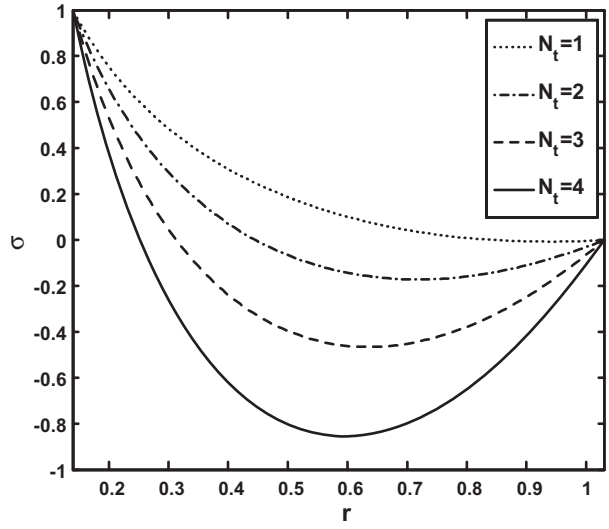

Fig. 5 Nanoparticles concentration profile for $z = 0.26$, $N_b = 3.55, \phi = 0.03, \varepsilon = 0.14$.

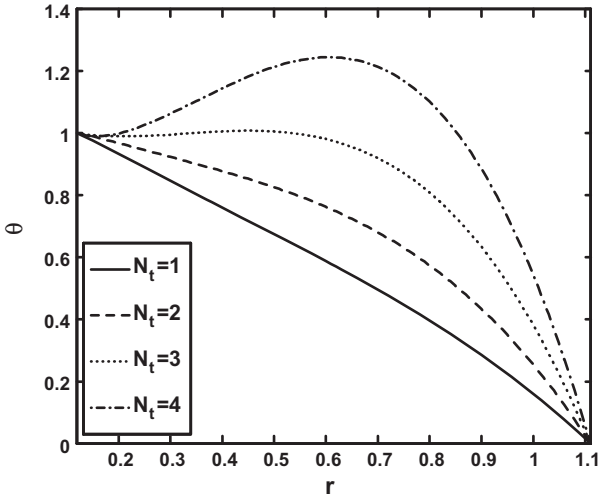

Fig. 7 Temperature profile for $z = 0.03, \varepsilon = 0.12, N_b = 1.83$, $\phi = 0.59$.

4. Square wave:

$$r_2(z) = 1 + \phi\left\{\frac{4}{\pi}\sum_{n=1}^{\infty}\frac{(-1)^{y+1}}{(2y-1)}\cos(2\pi(2y-1)z)\right\}. \tag{50}$$

5. Analytical solution by Adomian decomposition method

To develop the solution of Eqs. (31)–(33), we applied the Adomian decomposition method. We inscribe Eqs. (31)–(33) in the operator form as [32–37]

$$£_{r\sigma} + \frac{N_t}{N_b}£_{r\theta} = 0, \tag{51}$$

$$£_{r\theta} + N_b\frac{\partial\theta}{\partial r}\frac{\partial\sigma}{\partial r} + N_t\left(\frac{\partial\theta}{\partial r}\right)^2 = 0, \tag{52}$$

$$£_{rw} - \frac{\partial p}{\partial z} + \frac{1}{r}\frac{\partial}{\partial r}\left(rmWe\left(\frac{\partial w}{\partial r}\right)^2\right) + G_r\theta + B_r\sigma = 0. \tag{53}$$

The linear and the inverse operator are taken as

$$£_{\theta r} = £_{\sigma r} = \frac{1}{r}\frac{\partial}{\partial r}\left(r\frac{\partial}{\partial r}\right),\ £_{wr} = \frac{1}{r}\frac{\partial}{\partial r}\left(r(1-m)\frac{\partial}{\partial r}\right),$$
$$£_{\theta r}^{-1}[\cdot] = \int_{r_2}^{r}\left[\frac{1}{2}\int_{r_2}^{r}[\cdot]dr\right]dr,\ £_{\sigma r}^{-1}[\cdot] = \int_{r_2}^{r}\left[\frac{1}{2}\int_{r_2}^{r}r[\cdot]dr\right]dr, \tag{54}$$
$$£_{wr}^{-1}[\cdot] = \int_{r_2}^{r}\left[\frac{1}{r(1-m)}\int_{r_2}^{r}r[\cdot]dr\right]dr$$

Applying $£_r^{-1}$ to the Eqs. (51)–(53) yields

$$\sigma(r,z) = \sigma_{20}(r,z) - \frac{N_t}{N_b}[\theta(r,z) - \theta_{20}(r,z)], \tag{55}$$

$$\theta(r,z) = \theta_{20}(r,z) - \int_{r_2}^{r}\left[\frac{1}{r}\int_{r_2}^{r}r\left[N_b\frac{\partial\theta}{\partial r}\frac{\partial\sigma}{\partial r}\right]dr\right]dr$$
$$- \int_{r_2}^{r}\left[\frac{1}{r}\int_{r_2}^{r}r\left[N_t\left(\frac{\partial\theta}{\partial r}\right)^2\right]dr\right]dr, \tag{56}$$

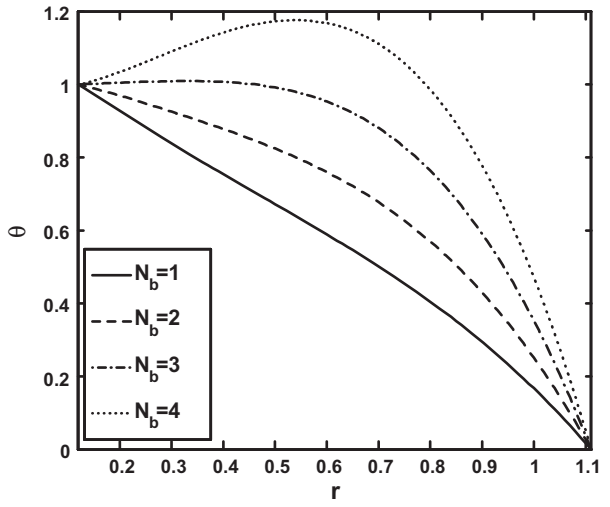

Fig. 8 Temperature profile for $z = 0.03, N_t = 1.83, \phi = 0.59, \varepsilon = 0.12$.

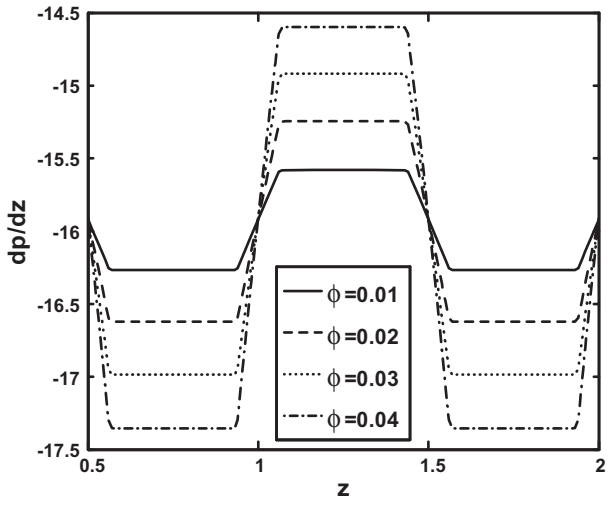

Fig. 10 Pressure gradient for (trapezoidal wave) for $m = 0.23$, $We = 0.13, B_r = 2.77, \varepsilon = 0.11, Q = 0.42, N_t = 2.88, G_r = 2.44, N_b = 2.72$.

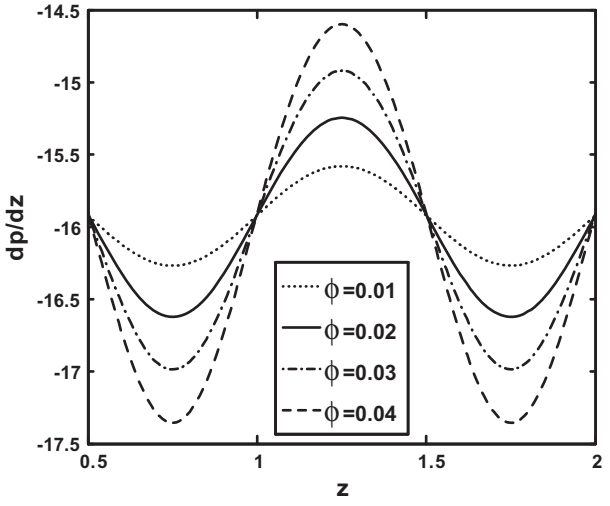

Fig. 9 Pressure gradient for sinusoidal wave for $m = 0.23$, $We = 0.13, B_r = 2.77, \varepsilon = 0.11, Q = 0.42, N_t = 2.88, G_r = 2.44, N_b = 2.72$.

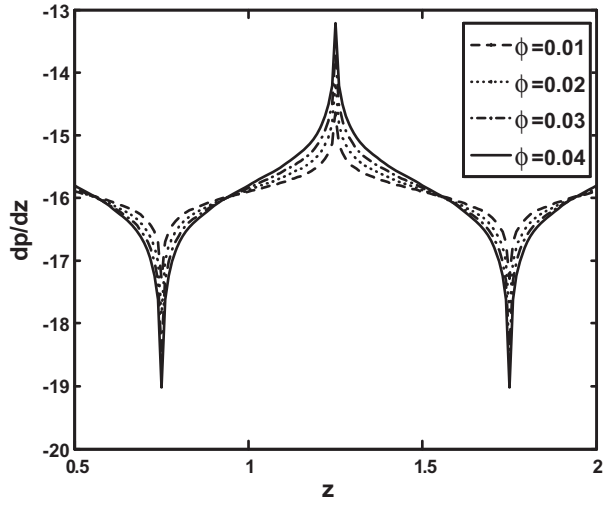

Fig. 11 Pressure gradient for (triangular wave) for $m = 0.23$, $We = 0.13, B_r = 2.77, \varepsilon = 0.11, Q = 0.42, N_t = 2.88, G_r = 2.44, N_b = 2.72$.

$$w(r,z) = w_{20}(r,z) + \int_{r_2}^{r}\left[\frac{1}{r(1-m)}\int_{r_2}^{r} r\left[\frac{\partial p}{\partial z}\right]dr\right]dr - \int_{r_2}^{r}\left[\frac{1}{r(1-m)}\int_{r_2}^{r} r\left[\frac{1}{r}\frac{\partial}{\partial r}\left(rmWe\left(\frac{\partial w}{\partial r}\right)^2\right)\right]dr\right]dr - \int_{r_2}^{r}\left[\frac{1}{r(1-m)}\int_{r_2}^{r} r[G_r\theta + B_r\sigma]dr\right]dr. \tag{57}$$

Now we decompose $\sigma,\ \theta$, w as

$$\sigma = \sum_{y=0}^{\infty}\sigma_y,\ \theta = \sum_{y=0}^{\infty}\theta_y,\ w = \sum_{y=0}^{\infty}w_y \tag{58}$$

Making use of Eq. (58) the solutions of Eqs. (55)–(57) are finally defined as

$$\sigma = -\frac{N_t}{N_b}\left(\frac{r-r_2}{r_1-r_2}\right) + C_1\ln r + C_2 + \ldots, \tag{59}$$

$$\theta = -\frac{N_t}{N_b}\left(\frac{r-r_2}{r_1-r_2}\right) + C_3\ln r + C_4 + r^2 b_8 + r b_9 + b_{10}\ln r + b_{11}(\ln r)^2 + b_{12} + \ldots, \tag{60}$$

$$w = a_1\ln r + a_2 + \frac{1}{2(1-m)}\frac{dp}{dz}\left(\frac{r^2}{2} - r_2^2\ln r + b_{18}\right) - r^3 b_{21} - r^2 b_{22} - b_{23}r^2\ln r + b_{24}\ln r + b_{25} + \ldots, \tag{61}$$

where non-linear term is solved by Adomian Polynomial and constants C_1 to C_4 and $a_1,\ a_2$ are evaluated by using the following conditions:

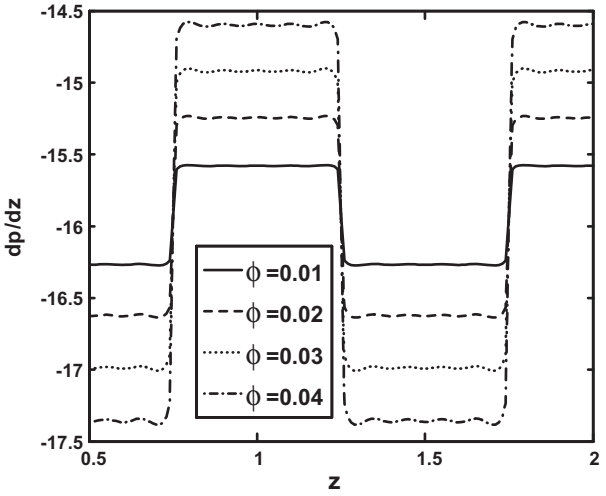

Fig. 12 Pressure gradient for (square wave) for $m = 0.23$, $We = 0.13, B_r = 2.77, \varepsilon = 0.11, Q = 0.42, N_t = 2.88, G_r = 2.44, N_b = 2.72$.

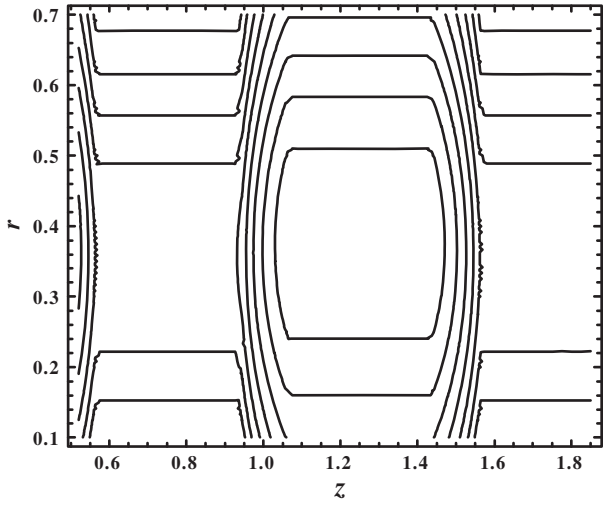

Fig. 14 Streamlines (Trapezoidal wave) for $N_t = 3.92, \phi = 0.10$, $m = 0.19, \varepsilon = 0.25, We = 0.11, N_b = 5.83, B_r = 5.22, Q = 0.53$, $G_r = 4.44, d = 1.4$.

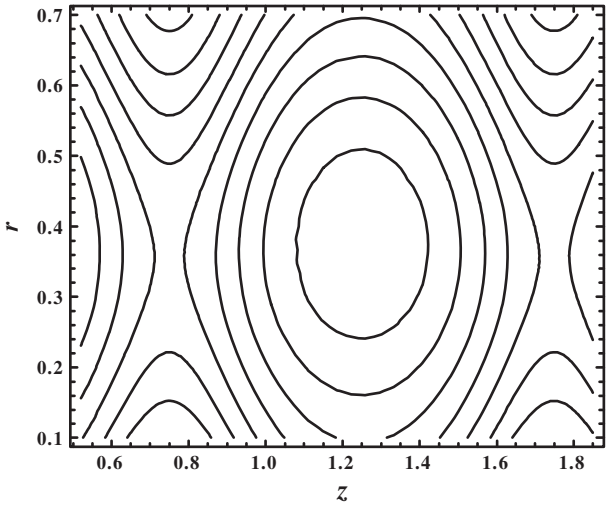

Fig. 13 Streamlines (sinusoidal wave) for $N_t = 3.92, \phi = 0.10$, $m = 0.19, \varepsilon = 0.25, We = 0.11, N_b = 5.83, B_r = 5.22, Q = 0.53, G_r = 4.44, d = 1.4$.

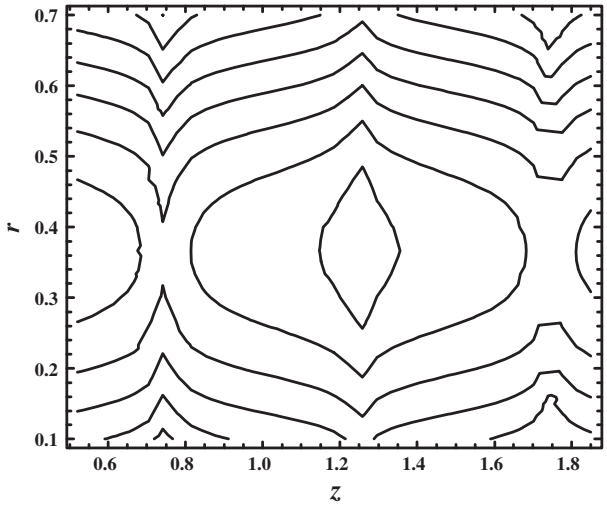

Fig. 15 Streamlines (Triangular wave) for $N_t = 3.92, \phi = 0.10$, $m = 0.19, \varepsilon = 0.25, We = 0.11, N_b = 5.83, B_r = 5.22, Q = 0.53, G_r = 4.44$.

$$\begin{aligned} &\theta = \sigma = 1 \text{ at } r = r_1, \\ &\theta = \sigma = 0 \text{ at } r = r_2 = 1 + \phi \sin 2\pi z, \\ &w = -1 \text{ at } r = r_1, \\ &w = -1 \text{ at } r = r_2 = 1 + \phi \sin 2\pi z. \end{aligned} \tag{62}$$

whereas all the constants are defined in Appendix A.

6. Results and discussion

We analyzed pressure rise, temperature, nanoparticles concentration, pressure gradient, and streamlines in this unit. Figs. 2–16 are shown for this purpose. Numerical integration is performed by using mathematics software to calculate pressure rise Δp. Fig. 1 shows the comparison of velocity profile for Homotopy perturbation Method (HPM) and Adomian Decomposition Method (ADM). Both techniques avoid linearization and other assumptions. The solutions arrived by HPM are much easier as compared to (ADM). To understand the feasibility of this method more terms of series are calculated. Accuracy increases if more components are included in the series, but at the expense of large increase in the difficulty of calculations. Pressure rise for various physical parameters such as We (Weissenberg number), N_t (thermophoresis parameter), and N_b (Brownian motion parameter) is observed in Figs. 2–4. Pumping characteristics known as retrograde pumping ($Q < 0, \Delta p > 0$), peristaltic pumping ($Q > 0, \Delta p > 0$) and augmented pumping ($Q > 0, \Delta p < 0$) are shown in Fig. 2 by the intervals $Q\varepsilon[-2, 0]$, $Q\varepsilon[0.01, 0.09]$, $Q\varepsilon[0.1, 2]$ respectively. One may observe from Fig. 2 that pressure rise decreases by

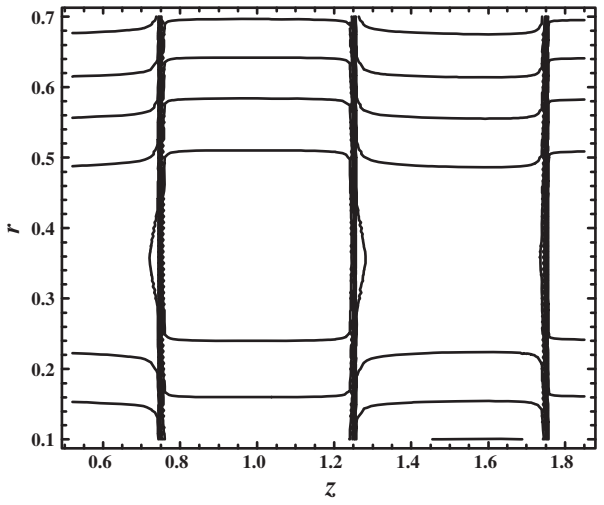

Fig. 16 Streamlines (Square wave) for $N_t = 3.92, \phi = 0.10, m = 0.19, \varepsilon = 0.25, We = 0.11, N_b = 5.83, B_r = 5.22, Q = 0.53, G_r = 4.44$.

increasing the values of We in retrograde pumping whereas opposite results are revealed in the augmented pumping region. Free pumping region ($Q = 0, \Delta p = 0$) can also be seen in Fig. 2. It is observed from Figs. 3 and 4 that by increasing values of N_b and N_t pressure rise increases in peristaltic, retrograde and augmented pumping regions. Variation of nanoparticles concentration profile for different values of N_t and N_b is displayed in Figs. 5 and 6. It is observed that with the increase of N_t nanoparticles concentration decreases; however, nanoparticles concentration increases with the increase of N_b. Figs. 7 and 8 present the variation of temperature profile for different values of N_t and N_b. Temperature profile increases by increasing values of N_t and N_b. The deviation of pressure gradient for different values of ϕ is described in Figs. 9–12. These figures show that in the wider part of the annulus in the regions ($z\varepsilon$ [0.5, 1], $z\varepsilon$ [1.5, 2]) for Figs. 9–11 and ($z\varepsilon$ [0.5, 0.75], $z\varepsilon$ [1.26, 1.75]) for Fig. 12 pressure gradient is small. It means that the flow can easily pass without imposition of large pressure gradient. On the other hand large pressure gradient occurs in the narrow portion of the annulus shown by the regions ($z\varepsilon$ [1.1, 1.49] for Figs. 9–11 and ($z\varepsilon$ [0.76, 1.25] for Fig. 12). It means that in this region large pressure gradient is required to maintain the same flux to pass it. This is in good agreement with the physical situation. The trapping occurrence for four different waveforms can be seen in Figs. 13–16. It is depicted that the size of the trapped bolus in triangular wave is smaller as associated with the other waves.

7. Conclusions

This study examines the effects of nanoparticles on the peristaltic flow of hyperbolic tangent fluid in an annulus. The leading points of the phenomenon are given as follows:

(1) For increasing values of N_b and N_t retrograde, peristaltic and augmented pumping increases.
(2) Temperature profile increases with an increase in N_t and N_b.
(3) Nanoparticles concentration declines with the increase in N_t and increases with increase in N_b.
(4) Pressure gradient takes the form of the wave which is taken into account.
(5) The size of trapped bolus in triangular wave is smaller as compared to the other waves.

Appendix A.

$$\ell_{11} = r_1 - r_2, \ell_{12} = \frac{r_2}{\ell_{11}}, \ell_{13} = N_t + N_b, \ell_{13'} = 2N_t + N_b, \ell_{14} = \ln r_1 - \ln r_2,$$
$$\ell_{15} = r_2^2 - r_1^2, \ell_{16} = \frac{-\ell_{13}}{4\ell_{11}^2}, \ell_{17} = \frac{1}{\ell_{14}} + \frac{\ell_{15}\ell_{16}}{\ell_{14}}, \ell_{18} = r_2^2 \ln r_1 - r_1^2 \ln r_2,$$
$$\ell_{19} = \frac{-\ln r_2}{\ell_{14}} - \frac{\ell_{16}\ell_{18}}{\ell_{14}}, \ell_{20} = \ell_{12} + \ell_{19}, \ell_{21} = \frac{-\ell_{13}}{N_b \ell_{11}}, \ell_{22} = \frac{\ell_{12}\ell_{13}}{N_b},$$
$$\ell_{23} = \frac{-\ell_{21}\ell_{11}}{\ell_{14}}, \ell_{24} = r_1 \ln r_2 - r_2 \ln r_1, \ell_{25} = \frac{\ell_{21}\ell_{24}}{\ell_{14}} - \ell_{22}, \ell_{26} = \ell_{22} + \ell_{25},$$
$$\ell_{27} = \frac{-N_t}{N_b}, \ell_{28} = \ell_{16}\ell_{27}, \ell_{29} = \frac{\ell_{27}}{\ell_{11}}, \ell_{30} = \ell_{17}\ell_{27}, \ell_{31} = \ell_{20}\ell_{27},$$
$$\ell_{32} = (\ell_{15}\ell_{28} + \ell_{11}\ell_{29} - \ell_{14}\ell_{30})/\ell_{14}, \ell_{33} = -(\ell_{18}\ell_{28} + \ell_{24}\ell_{29} + \ell_{14}\ell_{31})/\ell_{14}, \ell_{34}$$
$$= \ell_{30} + \ell_{32}, \ell_{35} = \ell_{31} + \ell_{33}, \ell_{36} = \frac{1}{\ell_{11}} + \ell_{21} - \ell_{29}, \ell_{37} = \ell_{23} + \ell_{34},$$
$$\ell_{38} = \ell_{26} - \ell_{12} + \ell_{35}, \ell_{39} = \frac{-2\ell_{13'}\ell_{16}}{9\ell_{11}}, \ell_{40} = \frac{-\ell_{13'}}{4\ell_{11}^2} + \frac{N_b\ell_{21}}{4\ell_{11}},$$
$$\ell_{41} = \frac{-\ell_{13'}\ell_{17}}{\ell_{11}} - \frac{N_b\ell_{23}}{\ell_{11}}, \ell_{42} = r_1^3 - r_2^3, \ell_{43} = \frac{-\ell_{39}\ell_{42} - \ell_{15}\ell_{40} - \ell_{11}\ell_{41}}{\ell_{14}},$$
$$\ell_{44} = r_1^3 \ln r_2 - r_2^3 \ln r_1, \ell_{45} = \frac{\ell_{39}\ell_{44} + \ell_{18}\ell_{40} + \ell_{24}\ell_{41}}{\ell_{14}}, \ell_{46} = \ell_{16} - \ell_{40},$$
$$\ell_{47} = \ell_{17} + \ell_{43}, \ell_{48} = -\ell_{12} + \ell_{20} + \ell_{45}, \ell_{49} = \frac{-(r_1^2 - r_2^2)}{4(1-m)\ell_{14}}, \ell_{50} = \frac{(r_1^2 \ln r_2 - r_2^2 \ln r_1)}{4(1-m)\ell_{14}},$$
$$\ell_{51} = \frac{-nWe}{12(1-m)^3}\left(\frac{dp_0}{dz}\right)^2 - \frac{G_r + B_r}{9\ell_{11}(1-m)}, \ell_{52} = \frac{(G_r + B_r)\ell_{12}}{4(1-n)} - \frac{1}{4(1-m)}\frac{dp_0}{dz},$$
$$\ell_{53} = \frac{-nWe\ell_{49}}{(1-m)^2}\left(\frac{dp_0}{dz}\right)^2, \ell_{54} = \frac{nWe\ell_{49}^2}{(1-m)}\left(\frac{dp_0}{dz}\right)^2, \ell_{55} = -\ell_{49}\frac{dp_0}{dz}, \ell_{56} = 1 - \ell_{50}\frac{dp_0}{dz},$$
$$\ell_{57} = \frac{-(1-m)}{\ell_{14}}(\ell_{51}(r_1^3 - r_2^3) + \ell_{52}(r_1^2 - r_2^2) + \ell_{53}(r_1 - r_2)$$
$$+ \ell_{54}\left(\frac{1}{r_1} - \frac{1}{r_2}\right) + \ell_{55}(\ln r_1 - \ln r_2)),$$
$$\ell_{58} = \frac{1}{\ell_{14}}(\ell_{51}(r_1^3 \ln r_2 - r_2^3 \ln r_1) + \ell_{52}(r_1^2 \ln r_2 - r_2^2 \ln r_1)$$
$$+ \ell_{53}(r_1 \ln r_2 - r_2 \ln r_1) + \ell_{54}\left(\frac{\ln r_2}{r_1} - \frac{\ln r_1}{r_2}\right) + \ell_{56}(\ln r_2 - \ln r_1)),$$
$$\ell_{59} = \ell_{55} + \frac{\ell_{57}}{(1-m)}, \ell_{60} = \ell_{56} + \ell_{58}, \ell_{61} = \frac{3\ell_{51}}{2(1-m)}\frac{dp_0}{dz},$$
$$\ell_{62} = \frac{\ell_{52}}{(1-n)}\frac{dp_0}{dz} + \frac{dP_0}{dz}\frac{dp_1}{dz}\frac{1}{4(1-m)^2}, \ell_{63} = \frac{\ell_{53}}{2(1-m)}\frac{dp_0}{dz} + 3\ell_{49}\ell_{51}\frac{dp_0}{dz},$$
$$\ell_{64} = \frac{\ell_{59}}{2(1-m)}\frac{dp_0}{dz} + \frac{dp_0}{dz}\frac{dp_1}{dz}\frac{\ell_{49}}{(1-m)} + 2\ell_{49}\ell_{52}\frac{dp_0}{dz}, \ell_{65} = -\frac{\ell_{54}}{2(1-m)}\frac{dp_0}{dz} + \ell_{49}\ell_{53}\frac{dp_0}{dz},$$
$$\ell_{66} = \ell_{49}^2\frac{dp_0}{dz}\frac{dp_1}{dz} + \ell_{49}\ell_{59}\frac{dp_0}{dz}, \ell_{67} = -\ell_{49}\ell_{54}\frac{dp_0}{dz}, \ell_{68} = \frac{-2mWe\ell_{61}}{4(1-m)} - \frac{G_r\ell_{61}}{16(1-m)},$$
$$\ell_{69} = \frac{-2mWe\ell_{62}}{3(1-m)} + \frac{G_r}{9\ell_{11}(1-m)} - \frac{B_r\ell_{21}}{9(1-m)}, \ell_{70} = \frac{-mWe\ell_{63}}{(1-m)} + \frac{G_r\ell_{17}}{4(1-m)} - \frac{B_r\ell_{26}}{4(1-m)} - \frac{G_r\ell_{20}}{4(1-m)} + \frac{B_r\ell_{23}}{4(1-m)},$$
$$\ell_{71} = \frac{-2mWe\ell_{64}}{(1-m)}, \ell_{72} = \frac{-2mWe\ell_{65}}{(1-m)}, \ell_{73} = \frac{-G_r\ell_{17}}{4(1-m)} - \frac{B_r\ell_{23}}{4(1-m)}, \ell_{74} = \frac{-2mWe\ell_{66}}{(1-m)},$$
$$l_{75} = \frac{-mWe\ell_{67}}{(1-m)}, \ell_{76} = \frac{-(1-m)}{\ell}$$
$$\ell_{71}(r_1 - r_2) + \ell_{72}(\ln r_1 - \ln r_2) + \ell_{73}(r_1^2 \ln r_1 - r_2^2 \ln r_2) + \ell_{74}\left(\frac{1}{r_2} - \frac{1}{r_1}\right)$$
$$+ \ell_{75}\left(\frac{1}{r_2^2} - \frac{1}{r_1^2}\right)), \ell_{77} = \frac{1}{\ell} + \ell_{71}(r_1 \ln r_2 - r_2 \ln r_1) + \ell_{73}(r_1^2 \ln r_1 \ln r_2 - r_2^2 \ln r_1 \ln r_2)$$
$$- \ell_{74}\left(\frac{\ln r_2}{r_1} - \frac{\ln r_1}{r_2}\right) + \ell_{75}\left(\frac{\ln r_1}{r_2^2} - \frac{\ln r_2}{r_1^2}\right)),$$
$$\ell_{78} = \ell_{72} + \frac{l_{74}}{1-m}, \ell_{79} = \ell_{69} + \ell_{51}, \ell_{80} = \ell_{52} + \ell_{70}, \ell_{81} = \ell_{53} + \ell_{71}, \ell_{82} = \ell_{54} - \ell_{74},$$
$$\ell_{83} = \ell_{59} + \ell_{78}, \ell_{84} = \ell_{60} + \ell_{77}, \ell_{85} = \frac{r_2^2 - r_1^2}{2}, \ell_{86} = \frac{r_2^4 - r_1^4}{16(1-m)}$$
$$+ \ell_{49}\left(\left(\frac{r_2^2 \ln r_2}{2} - \frac{r_2^2}{4}\right) - \left(\frac{r_1^2 \ln r_1}{2} - \frac{r_1^2}{4}\right)\right) + \ell_{50}\left(\frac{r_2^2 - r_1^2}{2}\right),$$
$$\ell_{87} = \frac{l_{51}}{5}(r_2^5 - r_1^5) + \frac{l_{52}}{4}(r_2^4 - r_1^4) + \frac{l_{53}}{3}(r_2^3 - r_1^3) + \ell_{54}(r_2 - r_1)$$
$$+ l_{59}\left(\left(\frac{r_2^2 \ln r_2}{2} - \frac{r_1^2 \ln r_1}{2}\right) - \left(\frac{r_2^2 - r_1^2}{4}\right) + \frac{l_{60}(r_2^2 - r_1^2)}{2}\right),$$
$$\ell_{88} = \frac{l_{68}}{6}(r_2^6 - r_1^6) + \frac{l_{69}}{5}(r_2^5 - r_1^5) + \frac{l_{70}}{4}(r_2^4 - r_1^4) + \frac{l_{71}}{3}(r_2^3 - r_1^3) + \frac{l_{77}}{2}(r_2^2 - r_1^2)$$
$$+ \ell_{78}\left(\left(\frac{r_2^2 \ln r_2}{2} - \frac{r_1^2 \ln r_1}{2}\right) - \left(\frac{r_2^2 - r_1^2}{4}\right)\right) + \ell_{73}\left(\left(\frac{r_2^4 \ln r_2}{4} - \frac{r_1^4 \ln r_1}{4}\right) - \left(\frac{r_2^4 - r_1^4}{16}\right)\right)$$
$$- \ell_{74}(r_2 - r_1) - \ell_{75}(\ln r_2 - \ln r_1),$$
$$l_{89} = \frac{l_{85} - l_{87} - l_{88}}{l_{86}}$$
$$b_1 = \left(\frac{-N_t}{N_b(r_1 - r_2)}\right)^2, b_2 = \frac{-2C_3N_t}{N_b(r_1 - r_2)}, b_3 = \frac{-N_t}{N_b(r_1 - r_2)}, b_4 = \frac{-r_2^2}{2}b_3^2 - r_2(C_1b_3 + C_3b_3)$$

$-C_1C_3(\ln r_2), b_5=\frac{-r_2^2}{4}b_3^2-r_2(C_1b_3+C_3b_3)-\frac{C_1C_3(\ln r_2)^2}{2}-b_4\ln r_2,\Big)$

$b_6=\frac{-b_1}{2}r_2^2-C_3^2(\ln r_2)-b_2r_2, b_7=\frac{-b_1}{4}r_2^2-\frac{C_3^2(\ln r_2)^2}{2}-b_2r_2-b_6\ln r_2,$

$b_8=\frac{-N_bb_3^2}{4}-\frac{b_1}{4}N_t, b_9=-N_b(C_1b_3+C_3b_3)-b_2N_t, b_{10}=-N_bb_4-b_6N_t,$

$b_{11}=\frac{-N_bC_1C_3}{2}-\frac{N_tC_3^2}{2}, b_{12}=-N_bb_5-b_7N_t, b_{13}=\frac{-(G_r+B_r)N_t}{N_b(r_1-r_2)},$

$b_{14}=C_3G_r+C_1B_r, b_{15}=C_4G_r+C_2B_r, b_{16}=\frac{mWea_1^2}{1-m}, b_{17}=\frac{b_{16}}{r_2}+\frac{b_{16}}{r_2}\ln(r_2),$

$b_{18}=\frac{-r_2^2}{2}+r_2^2\ln(r_2), b_{19}=\frac{-r_2^3b_{13}}{3}-b_{14}\left(\frac{r_2^2\ln(r_2)}{2}-\frac{r_2^2}{4}\right)-\frac{b_{15}r_2^2}{2},$

$b_{20}=\frac{-r_2^3b_{13}}{9(1-m)}-\frac{b_{14}}{(1-m)}\left(\frac{r_2^2\ln(r_2)}{2}-\frac{r_2^2}{4}\right)-\frac{b_{15}r_2^2}{4(1-m)}-\frac{b_{19}\ln(r_2)}{(1-m)}, b_{21}=\frac{b_{13}}{9(1-m)},$

$b_{22}=\frac{b_{15}}{4(1-m)}-\frac{2b_{14}}{8(1-m)}, b_{23}=\frac{b_{14}}{4(1-m)}, b_{24}=\frac{b_{16}}{r_2}-\frac{b_{19}}{(1-m)}, b_{25}=-b_{17}-b_{20}.$

References

[1] T.W. Latham, Fluid Motion in a Peristaltic Pump, MS Thesis, Massachusetts Institute of Technology, Cambridge, 1966.

[2] A.H. Shapiro, M.Y. Jafferin, S.L. Weinberg, Peristaltic pumping with long wavelengths at low Reynolds number, J. Fluid. Mech. 35 (1969) 669.

[3] J.C. Burns, T. Parkes, Peristaltic motion, J. Fluid. Mech. 29 (1967) 731.

[4] C. Barton, S. Raynor, Peristaltic flow in tubes, Bull. Math. Biophys. 30 (1968) 663.

[5] Y.C. Fung, C.S. Yih, Peristaltic transport, J. Appl. Mech. 35 (1968) 669.

[6] M. Ealshahed, M.H. Haroun, Peristaltic transport of Johnson–Segalman fluid under effect of a magnetic field, Math. Prob. Eng. 6 (2005) 663.

[7] Kh. S. Mekheimer, Y. Abd Elmaboud, Peristaltic flow of a couple stress fluid in an annulus; application of an endoscope, Physica A 387 (2008) 2403.

[8] S. Nadeem, S. Akram, Peristaltic flow of a Williamson fluid in an asymmetric channel, Commun. Nonlinear Sci. Numer. Simul. 15 (2010) 1705.

[9] M.H. Haroun, Effect of Deborah number and phase difference on peristaltic transport of a third order fluid in an asymmetric channel, Commun. Nonlinear Sci. Numer. Simul. 4 (2007) 463.

[10] M. Kothandapani, S. Srinivas, Peristaltic Transport of a Jeffrey fluid under the effect of magnetic field in an asymmetric channel, Int. J. Non-Linear Mech. 43 (2008) 915.

[11] S. Nadeem, N.S. Akbar, Series solutions for the peristaltic flow of a Tangent hyperbolic fluid in a uniform inclined tube, Z. Naturforsch. 65a (2010) 887.

[12] D. Tripathi, S.K. Pandey, S. Das, Peristaltic flow of viscoelastic fluid with fractional maxwell model through a channel, Appl. Math. Comput. 215 (2010) 3645.

[13] S. Nadeem, H. Sadaf, N.S. Akbar, Analysis of peristaltic flow for a Prandtl fluid model in an endoscope, J. Power Technol. 94 (2014) 1.

[14] S.U.S. Choi, Enhancing thermal conductivity of fluids with nanoparticles, in: D.A. Siginer, H.P. Wang (Eds.), Developments and Applications of Non-Newtonian Flows, vol. 66, ASME, New York, 1995, p. 99.

[15] J. Buongiorno, Convective transport in nanofluids, J. Heat Transfer 128 (2005) 240.

[16] A.V. Kuznetsov, D.A. Nield, Natural convective boundary-layer flow of a nanofluid past a vertical plate, Int. J. Thermal Sci. 49 (2010) 243.

[17] K. Sadik, A. Pramuanjaroenkij, Review of convective heat transfer enhancement with nanofluids, Int. J. Heat Mass Transfer 52 (2009) 3187.

[18] W.A. Khan, I. Pop, Boundary-layer flow of a nanofluid past a stretching sheet, Int. J. Heat Mass Transfer 53 (2010) 2477.

[19] S.E.B. Marga, S.J. Palm, C.T. Nguyen, G. Roy, N. Galanis, Heat transfer enhancement by using nanofluids in forced convection flows, Int. J. Heat Fluid Flow 26 (2005) 530.

[20] P. Rana, R. Bhargava, Flow and heat transfer of a nanofluid over a nonlinearly stretching sheet: a numerical study, Comm. Nonlinear Sci. Numer. Simul. 17 (2012) 212.

[21] N.S. Akbar, S. Nadeem, Endoscopic effects on the peristaltic flow of a nanofluid, Commun. Theor. Phys. 56 (2011) 761.

[22] S. Nadeem, H. Sadaf, A.M. Sadiq, Analysis of nanoparticles on peristaltic flow of prandtl fluid model in an endoscopy, Current Nanosci. 10 (2014) 709.

[23] Ellahi R, Riaz A, Nadeem S. A theoretical study of Prandtl nanofluid in a rectangular duct through peristaltic transport, Appl. Nanosci. doi: http://dx.doi.org/10.1007/s13204-013-0255-4.

[24] R. Ellahi, A. Riaz, S. Nadeem, M. Ali, Peristaltic flow of carreau fluid in a rectangular duct through a porous medium, Math. Probl. Eng. doi: http://dx.doi.org/10.1155/2012/329639.

[25] J.H. He, Application of homotopy perturbation method to nonlinear wave equations, Chaos Solitons Fract. 26 (2005) 695.

[26] J.H. He, Homotopy perturbation technique, a new nonlinear analytical technique, Comput. Methods Appl. 135 (2003) 73.

[27] F. Shakeri, M. Dehghan, Solution of delay differential equations via a homotopy perturbation method, Math. Comput. Model 48 (2008) 486.

[28] M. Dehghan, F. Shakeri, Solution of an integro-differential equation arising in oscillating magnetic fields using He's homotopy perturbation method, Prog. Electr. Res. PIER 78 (2008) 361.

[29] M. Dehghan, F. Shakeri, Use of He's homotopy perturbation method for solving a partial differential equation arising in modeling of flow in porous media, J. Porous Media 11 (2008) 765.

[30] A. Saadatmandi, M. Dehghan, A. Eftekhari, Application of He's homotopy perturbation method for non-linear system of second-order boundary value problems, Nonlinear Anal.: Real World Appl. 10 (2009) 1912.

[31] F. Soltanian, M. Dehghan, S.M. Karbassi, Solution of the differential-algebraic equations via homotopy perturbation method and their engineering applications, Int. J. Comput. Math. 87 (2010) 1950.

[32] A.M. Wazwaz, A reliable modification of Adomion Decomposition method, Appl. Math. Comput. 102 (1999) 77.

[33] A.M. Wazwaz, The modified of Adomion Decomposition method for analytical treatment of differential equation, Appl. Math. Comput. 173 (2006) 165.

[34] M. Dehghan, R. Salehi, Solution of a nonlinear time-delay model in biology via semi-analytical approaches, Comput. Phys. Commun. 81 (2010) 1255.

[35] N.T. Eldabe, E.M. Elghazy, A. Ebaid, Closed form solution to a second order boundary value problem and its application in fluid mechanics, Phys. Lett. A 363 (2007) 257.

[36] F. Shakeri, M. Dehghan, Application of the decomposition method of Adomian for solving the pantograph equation of order m, Z. Naturforsch. A 65a (2010) 453.

[37] M. Dehghan, M. Tatarib, Finding approximate solutions for a class of third-order non-linear boundary value problems via the decomposition method of Adomian, Int. J. Comput. Math. 87 (2010) 1256.